

The Optic Nerve Head as a Robust Biomechanical System

Ian A. Sigal,^{1,2,3} Richard A. Bilonick,¹ Larry Kagemann,^{1,3} Gadi Wollstein,^{1,4}
Hiroshi Ishikawa,^{1,3} Joel S. Schuman,^{1,2,3,4} and Jonathan L. Grimm¹

PURPOSE. Understanding the effects of IOP on the optic nerve head (ONH) is important in understanding glaucoma and ONH structure and function. The authors tested the hypothesis that the ONH is a robust biomechanical structure wherein various factors combine to produce a relatively stable response to IOP.

METHODS. The authors generated two populations of 100,000 ONH numerical models each with randomly selected values, but controlled distributions, either uniform or Gaussian, of ONH geometry and mechanical properties. The authors predicted the lamina cribrosa displacement (LCD), scleral canal expansion (SCE), and the stresses (forces) and deformations (strains) produced by a 10 mm Hg increase in IOP. The authors analyzed the distributions of the responses.

RESULTS. The responses were distributed nonuniformly, with the majority of the models having a response within a small region, often less than 30% of the size of the overall response region. This concentration of responses was more marked in the Gaussian population than in the uniform population. All the responses were positively skewed. Whether a particular case was typical or not depended on the response used for classification and on whether the decision was made using one-dimensional or two-dimensional criteria.

CONCLUSIONS. Despite wide variations in ONH characteristics and responses to IOP, some responses were much more common than others. This supports conceiving of the eye as a robust structure, particularly for LCD and SCE, which is tolerant to variations in tissue geometry and mechanical properties. The authors also provide the first estimates of the typical mechanical response of the ONH to variations in IOP over a large population of ONHs. (*Invest Ophthalmol Vis Sci* 2012;53:2658-2667) DOI:10.1167/iovs.11-9303

Glaucoma is one of the leading causes of blindness worldwide.¹ Although elevated intraocular pressure (IOP) is the primary risk factor for the development and progression of the disease, its effects on the tissues of the eye remain unclear. The lamina cribrosa (LC) within the scleral canal in the optic nerve head (ONH) is thought to be the primary site of axonal damage in glaucoma.^{2,3} Hence, understanding the effects of IOP on the ONH, and on the LC in particular, has been an interest for many years.^{1,3-6}

Both experimental^{3,7-11} and modeling^{5,12-20} studies have described effects of IOP on the ONH which are complex, involving multiple factors having nonlinear effects and which interact in complicated ways.^{12,13,21} The range of effects of IOP has been proposed to explain, at least in part, the differences in individual sensitivity to IOP whereby some individuals suffer from vision loss at normal levels of IOP whereas others remain apparently unaffected by elevated pressures.^{1,4}

Whilst this complexity has often been taken as a challenge for understanding the ONH, the authors propose instead to think of it as a valuable property emerging from the ONH being a robust biomechanical system. In other words, the authors propose that although there are multiple factors influencing the sensitivity of the ONH to IOP variations, the factor effects combine to produce a relatively stable response to IOP whereby the majority of the ONHs have responses within a relatively tight range. The goal of this study was to test this hypothesis by studying on a large population of ONHs the distribution of the IOP-induced anterior-posterior lamina cribrosa displacement (LCD), scleral canal expansion (SCE), forces (stress) and deformations (strain).

METHODS

The authors generated two populations of 100,000 ONH models each with randomly selected values, but controlled distributions, either uniform or Gaussian, of the following parameters (Fig. 1 and Table 1): scleral thickness and Young's modulus (stiffness), eye radius (internal radius of the scleral shell), lamina cribrosa radius, anterior-posterior position and Young's modulus, neural tissue Young's modulus and pre-laminar tissue compressibility. The eight parameters were identified in a previous sensitivity analysis as the most influential on ONH biomechanics from 21 originally considered parameters^{13,22} (Table 1). Parameter ranges corresponded to healthy subjects and were based on the literature.^{14,15} For the Gaussian population the standard deviations were chosen as one sixth of the range so that the vast majority of the cases (99.7%) were within the intended ranges. Cases with a parameter outside the chosen ranges were discarded. The biomechanical effects of a 10 mm Hg increase in IOP (from 5 to 15 mm Hg) were predicted for each case using a published surrogate model²² based on finite element models of the ONH¹³⁻¹⁵ (Fig. 1).

Ten aspects of the response of an ONH to increases in IOP were analyzed: LCD, SCE, laminar maximum and minimum principal strains (representing the maximum tissue stretch and compression, respectively), laminar maximum shear strain (computed as described

From the ¹Department of Ophthalmology, UPMC Eye Center, Eye and Ear Institute, Ophthalmology and Visual Science Research Center University of Pittsburgh School of Medicine, Pittsburgh, Pennsylvania; ²McGowan Institute for Regenerative Science, University of Pittsburgh School of Medicine, Pittsburgh, Pennsylvania; ³Department of Bioengineering, Swanson School of Engineering, University of Pittsburgh, Pittsburgh, Pennsylvania; and ⁴Fox Center for Vision Restoration of UPMC and the University of Pittsburgh, Pittsburgh, Pennsylvania.

Funding: Supported in part by National Institutes of Health Grant P30-EY008098 (Bethesda, Maryland); Eye and Ear Foundation (Pittsburgh, Pennsylvania); and unrestricted grants from Research to Prevent Blindness (New York, New York).

Submitted for publication December 12, 2011; revised February 14, 2012; accepted March 11, 2012.

Disclosure: **I.A. Sigal**, None; **R.A. Bilonick**, None; **L. Kagemann**, None; **G. Wollstein**, None; **H. Ishikawa**, None; **J.S. Schuman**, None; **J.L. Grimm**, None

Corresponding author: Ian A. Sigal, Ocular Biomechanics Laboratory, Department of Ophthalmology, UPMC Eye Center, Eye and Ear Institute, Ophthalmology and Visual Science Research Center, University of Pittsburgh School of Medicine, 203 Lothrop Street, Rm 930, Pittsburgh, PA 15213; sigalia@upmc.edu.

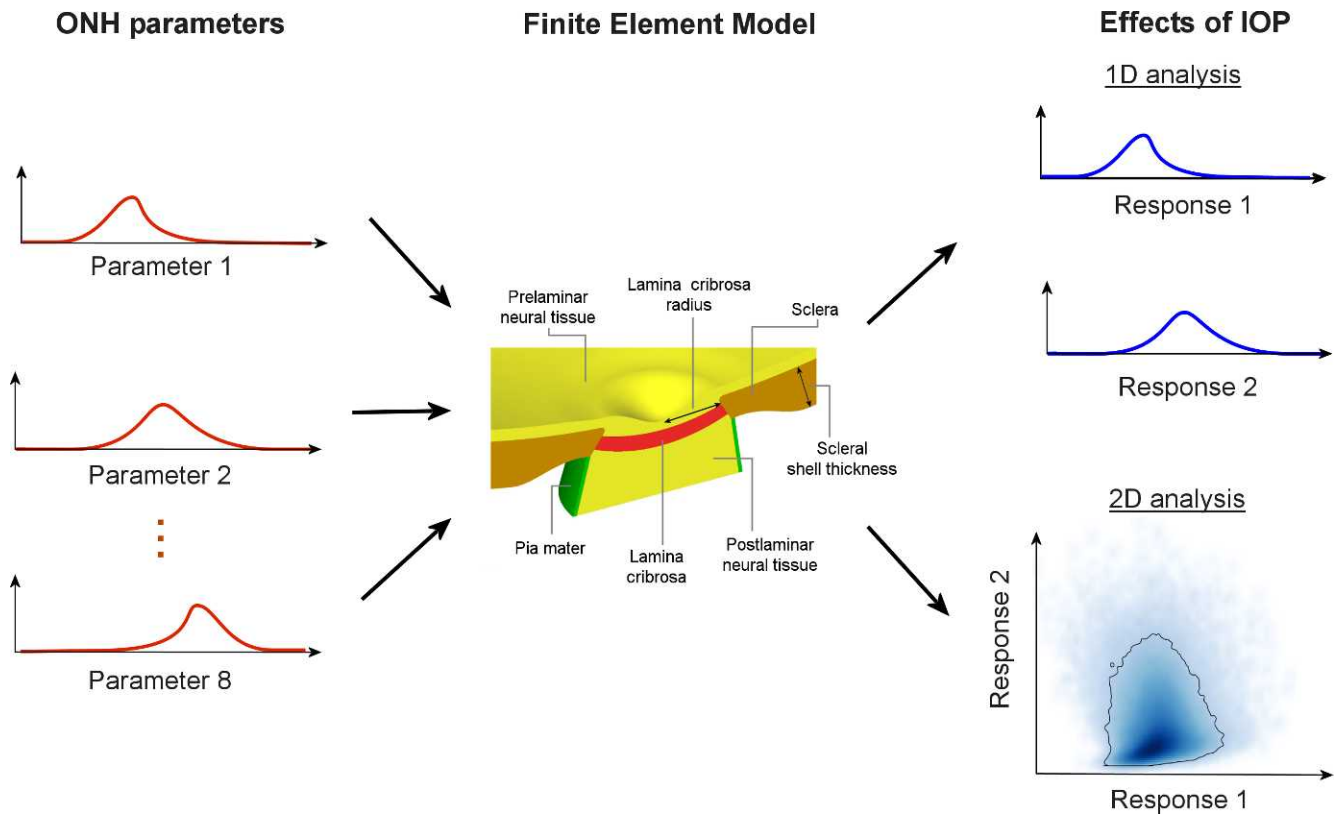


FIGURE 1. General strategy. The authors generated two cohorts each with 100,000 cases with controlled distributions of ONH parameters. Eight parameters were varied: eye radius, scleral thickness and modulus (stiffness), lamina cribrosa radius, position and modulus, and prelaminar tissue compressibility. An ONH model was created for each case and surrogate models based on finite element techniques used to predict the effects of an increase in IOP. The base model geometry corresponded to an IOP of 5 mm Hg. These effects were characterized by a set of responses. The distributions of the responses were analyzed one by one and in pairs. Five tissue regions were modeled: corneoscleral shell, LC, prelaminar neural tissue (PLNT, including the retina and choroid), postlaminar neural tissue (ON, including the optic nerve), and pia mater. IOP was represented as a homogeneous force on the interior surfaces. The apex of the anterior pole was constrained in all directions to prevent displacement or rotation. See Table 1 for the ONH parameters varied and their ranges.

elsewhere¹⁶) and the laminar von Mises stress (a measure of the forces carried by the tissue per unit area). Since the strains and stress vary over the tissues, for each of them the authors computed two measures to represent these distributions, namely the 50th and 95th percentiles which henceforth are referred to as median and peak. When analyzing the results the authors found that, although the magnitudes were different, the patterns obtained for the various measures of strain were similar to each other, as were the two measures of stress. Thus, for brevity, the results of only four responses are shown: LCD, SCE, median maximum principal strain, and median von Mises stress.

The authors analyzed the distribution of the responses using one-dimensional (1D) and two-dimensional (2D) criteria to determine the

regions with typical and atypical responses. Typical was defined as encompassing 95% of the cases, such that using 1D criteria the typical response range was the region between the 2.5 and 97.5 percentiles. Using 2D criteria the typical response range was the smallest region in 2D space enclosing 95% of the cases. As a measure of the concentration of responses the authors computed the ratio of typical to overall response ranges. To test the consequences of the choice of 95th percentile as the definition of typical the authors repeated the calculations of these ratios for percentiles from 0 to 100th every 5th percent.

The authors have reported on the sensitivity that the effects of IOP have on the characteristics of the ONH.^{13-15,23-25} Compared with the authors' previous studies,^{14,15,24,25} this work sampled the parameter space much more densely. It is possible that the factor influences on the responses reported depended on the parameter sampling strategy and the population size.²⁶ The current study leveraged the models produced for this work and recalculated the factor influences using the new populations of models. The effect of the parameter distributions was tested by defining population as a categorical factor with two levels (uniform or Gaussian), and computing the percentage contribution to the total sum of squares of each of the parameters and their interactions on each of the responses.^{13,26} For the sensitivity analysis the response variables were transformed to improve the normality of their distributions and of the residuals, satisfy the requirements of ANOVA, and allow factor effects to be added in an unbiased fashion. The authors used the Box-Cox method to verify that the transforma-

TABLE 1. Parameters, Their Ranges and Standard Deviations

Parameter	Mean	Low	High	SD
Internal eye radius (mm)	12.0	9.6	14.4	0.8
Scleral thickness (µm)	800	640	960	53
Scleral modulus (MPa)	5	1	9	1.33
Lamina cribrosa radius (µm)	950	760	1140	63.3
Lamina cribrosa position (µm)	100	0	200	33.3
Lamina cribrosa modulus (MPa)	0.5	0.1	0.9	0.133
Neural tissue modulus (MPa)	0.05	0.01	0.09	0.0133
Pre-laminar tissue compressibility (Poisson ratio)	0.45	0.4	0.49	0.015

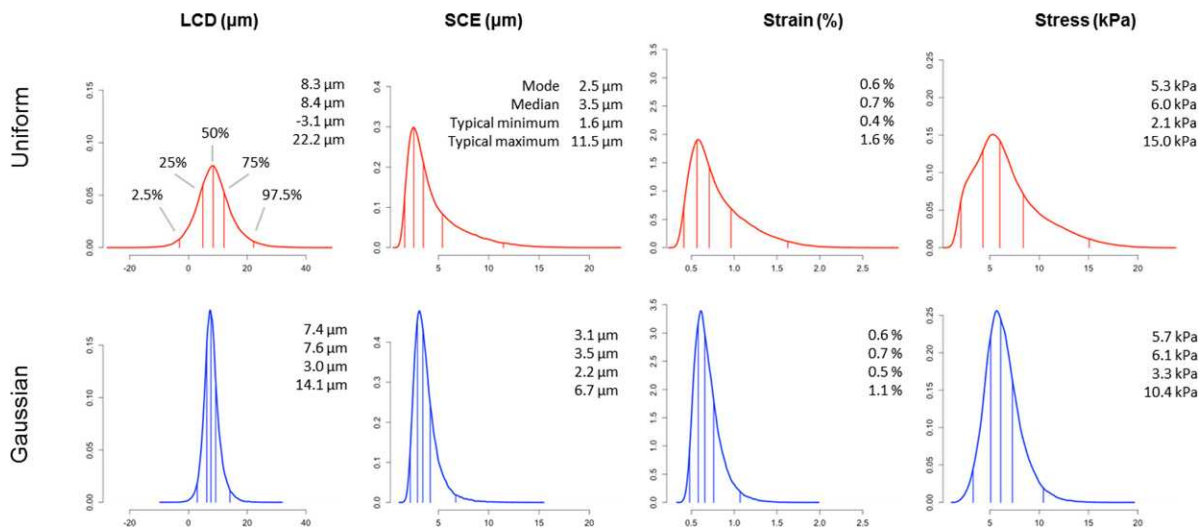


FIGURE 2. Uni-dimensional distribution of the responses. Distributions of IOP-induced LCD, SCE, median maximum principal (tensile) strain, and von Mises stress predicted for populations with ONH parameters with uniform (*top row*) or Gaussian (*bottom row*) distributions. The vertical lines in each of the plots are the 2.5, 25, 50, 75, and 97.5 percentiles. Next to each distribution are listed the mode, median, and the minimum and maximum of the limits of the typical range (in 1D defined as the region between the 2.5 to 97.5 percentiles) for that response and population. In both populations of ONHs a large fraction of the responses was concentrated within a relatively small region of the range of responses. This concentration was more marked for the Gaussian population than for the uniform population.

tions selected were simple and suitable.²⁶ The analyses were done using open-source software (R *v2.12.0* ²⁷).

RESULTS

The responses were distributed nonuniformly, with the majority of the models having a response within a small region of the overall response range (Fig. 2). Using 1D criteria the typical range (95% of the responses) of the distribution of LCD computed using the uniform population was 25.3 μm (−3.1–22.2 μm), which was just under 34.4% of an overall range of 73.5 μm (Table 2). For the Gaussian population this typical range decreased to 11.1 μm (3.0–14.1 μm), about 28% of an overall range of 40.4 μm. All the responses had similar distributions for both populations, with tighter typical ranges for the Gaussian population than for the uniform one. All the responses were positively skewed. LCD was the least skewed response, but it had

the largest difference between the medians of the populations. Response concentration was also obtained for the stress and strain, such that the typical regions were only 59.4% and 48.1% the size of the overall range for the uniform population, respectively, and 40.4% and 37.2% for the Gaussian population.

The concentration of responses was even more notable using 2D criteria (Fig. 3). The areas of the typical ranges when LCD and SCE were considered simultaneously were 57 μm² and 274 μm², for the Gaussian and uniform populations, respectively. These areas are 15% and 21% of the overall ranges of the responses. When the tensile strain and the stress were considered simultaneously, the areas of the typical ranges were 3.8 kPa and 12.1 kPa, for the Gaussian and uniform populations, respectively, which are 21% and 31% of the overall range of the responses. The concentration of responses in a relatively small region of the overall response range occurred for all responses, with both one-response and two-

TABLE 2. Overall and Typical Ranges for the Responses Independently and Paired, for a Definition of Typical Based on the 95% Most Common Responses

Response	Population	Overall Response Range	Typical Range (95th percentile)	Typical Range (95th percentile) Fraction (%)
LCD	Uniform	73.5 μm	25.3 μm	34.4
SCE	Uniform	21.5 μm	9.8 μm	45.7
LCD and SCE combined	Uniform	1326.2 μm ²	274.4 μm ²	20.7
Stress	Uniform	21.9 kPa	13.0 kPa	59.4
Strain	Uniform	2.5	1.2	48.1
Stress and Strain combined	Uniform	39.1 kPa	12.1 kPa	31.1
LCD	Gaussian	40.4 μm	11.1 μm	27.5
SCE	Gaussian	13.8 μm	4.5 μm	32.7
LCD and SCE combined	Gaussian	381.8 μm ²	57.2 μm ²	15.0
Stress	Gaussian	17.6 kPa	7.1 kPa	40.4
Strain	Gaussian	1.6	0.6	37.2
Stress and Strain combined	Gaussian	17.7 kPa	3.8 kPa	21.4

The rightmost column shows the ratio of the typical range to the overall range (%) as a measure of the concentration of the responses. Note that 10 responses were analyzed. For the reasons explained in the main text the results presented focus on four responses: LCD, SCE, the median maximum principal strain, and the median von Mises stress. For clarity these last two are referred to as Strain and Stress.

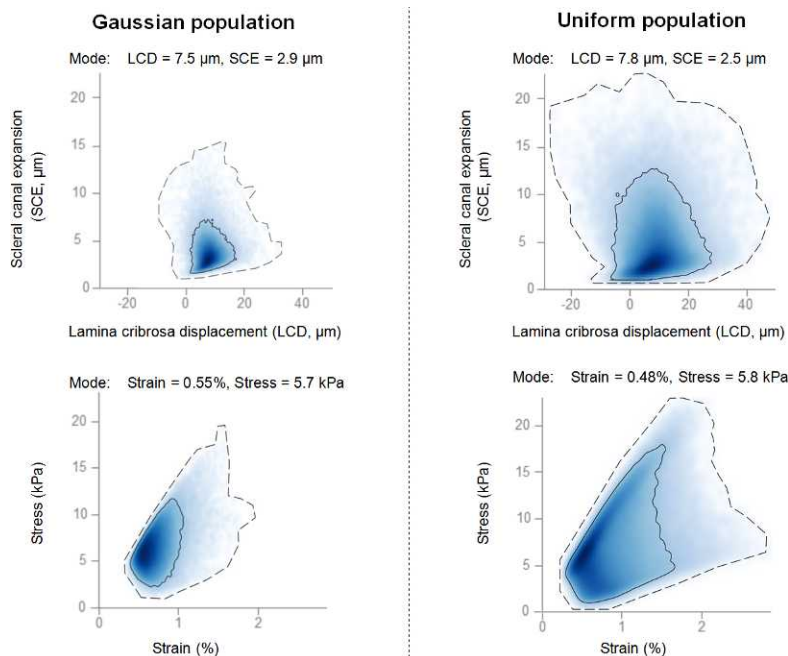


FIGURE 3. Two-dimensional distribution of the responses. Density plots of the 2D distributions of LCD and SCE (*top row*) or strain and stress (*bottom row*), computed for populations of ONHs with Gaussian (*left*) or uniform (*right*) parameter distributions. The plots are similar to 2D histograms in that dark/light areas represent regions with high/low frequency of responses. The dashed lines encompass all the responses, whereas the black lines are the outlines of the typical regions, defined in 2D as the smallest region encompassing 95% of the responses. The concentration of responses was even more marked than in the 1D distributions (Fig. 2). The region of typical responses has an odd shape that would have been difficult to predict using a small population. At low SCE's there was a sharp change in response densities, meaning that the boundary of the typical region was well defined and relatively insensitive to the percentile used to define what is typical. Elsewhere, the boundary of the typical region was more diffuse with only gradual changes in density, meaning that the boundary of the typical region was sensitive to the percentile used to define typical.

response criteria, and for any percent of cases (Fig. 4). The most concentrated responses were LCD, when considered independently, and LCD with SCE when considered simultaneously. The response modes were slightly different with the different criteria (Table 3).

The authors used scatterplots with the points colored by the main factors^{13,24} and responses to illustrate the relationships between factors and responses (Figs. 5, 6). The regions where the responses were concentrated typically included points of every color, meaning that no one parameter is sufficient to determine if a case would have a typical response or not. The boundaries of the regions of typical response varied from sharp (lower SCEs in Fig. 5) to diffuse (higher SCEs in Fig. 5). Whether a specific case was typical or not depended on the response used for the classification and on whether the decision was made using 1D or 2D criteria (Fig. 7).

Statistical analysis of the sensitivity of the responses on the parameters indicated that the choice of population only had a marginal influence on the parameter effects (Supplemental Figs. 1, 2). Population as a factor, independently and in interaction with other factors, accounted for less than 0.64%, 0.07%, 0.1%, and 1.2% of the variances in LCD, SCE, stress and strain, respectively.

DISCUSSION

The goal of this study was to test the hypothesis that despite wide variations in ONH characteristics and responses to IOP, some responses to IOP are much more common than others. The authors found that for all the measures a majority of the cases had responses concentrated within a relatively small region of the response range. This concentration was clear when the responses were analyzed independently and stronger

when two responses were considered simultaneously. LCD was more concentrated than any other independent effect of IOP. These results are important for three reasons.

Firstly, the results support conceiving the ONH as a robust biomechanical system which is tolerant to variations in geometry and tissue mechanical properties. The authors have shown that the factors affecting the ONH combine to maintain a relatively stable biomechanical sensitivity to IOP despite wide variations in tissue geometry and mechanical properties, such as a 9-fold increase in scleral stiffness. In the Gaussian population even the study's generous definition of typical produced responses concentrated within only 15% of the overall range of responses when using a two-response criteria (LCD and SCE). Although the concentration of responses was more marked in the population of ONHs with Gaussian distribution of parameters, it was still rather strong in the population with uniform distribution. This demonstrates that the concentration is a property of the response of the ONH to IOP and not a consequence of the assumed ONH characteristic distributions. The concept of the eye as a robust optical system was discussed in the elegant manuscript by Artal, Benito and Tabernero.²⁸ For the same population and percentile definition, the highest concentration of responses was found for LCD and SCE combined. Next were LCD and SCE independently, which were about as concentrated as the stress and strain combined, followed by the independent strain and stress. Independent strains were more concentrated than the stresses. These results can be interpreted as showing that the ONH is more robust as a structure first with respect to LCD, followed by SCE, then by strain and stress.

Secondly, this study has provided the first estimates of the typical mechanical responses of the ONH to variations in IOP over a large population of eyes. The results suggest that these

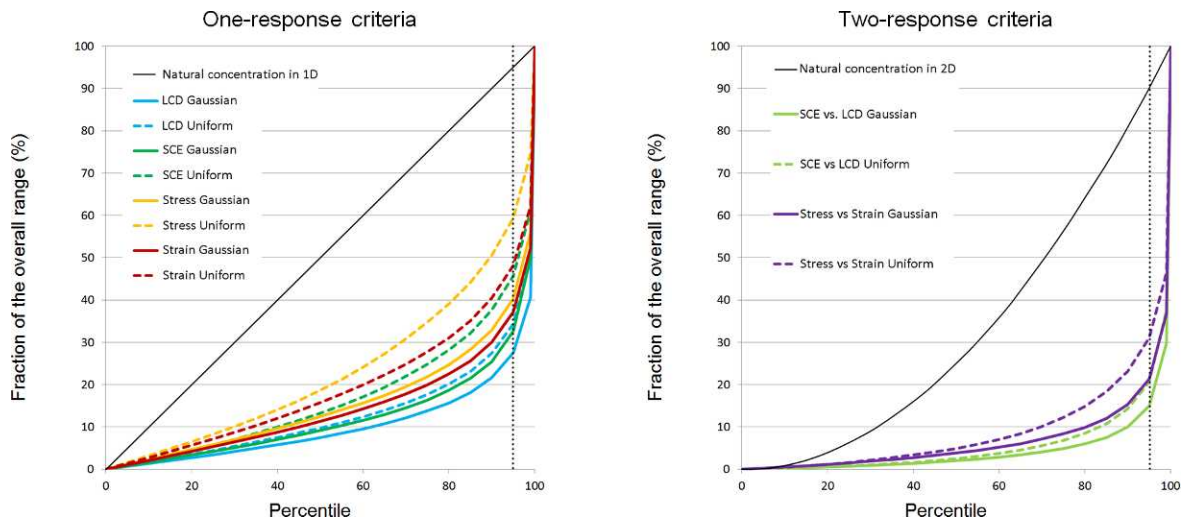


FIGURE 4. Concentration of the responses. As a measure of the concentration of the responses the authors computed the fraction of the overall range that a given percentile of responses spanned. The vertical dotted line represents the 95th percentile used elsewhere in this article to classify a response as typical. The use of a ratio allows fair comparison between responses with different units and scales, and between responses from different populations. A small fraction corresponds to a response where the fraction of cases is highly concentrated. The authors found that all the responses concentrated within a relatively small region of the overall response range, for both one-response (*left*) and two-response (*right*) criteria, irrespective of the population, although the strength of the population varied between responses, populations, and the percentile. For example, a definition based on LCD and SCE from the Gaussian population showed the strongest concentration, such that for any percentile below 90% the responses were concentrated within an area smaller than 10% of that of the overall response range. Using two-response criteria the 50% most common responses were concentrated within an area smaller than 6% of that of all the responses. The weakest concentration was for the stress from the uniform population. Using one-response criteria the 50% most common responses were concentrated within an area smaller than 18% of that of all the responses. The black lines represent the “natural” concentration of responses expected for the given percentile of responses and dimensionality. See the main text for a description of how this was computed. All the responses were more concentrated than the natural concentration for the given dimensionality, and therefore support the concept of robustness proposed in this work.

responses may not be normally distributed, and therefore that researchers should be cautious in the interpretation of experiments or simulations based on a few cases. The response distributions were positively skewed with a mode lower than the median. This is important because an experimental measurement is most likely to obtain the mode which would underestimate the median and the mean. The investigators defined the typical response as that encompassing 95% of the cases, which is equivalent to defining it as common, which is not necessarily the same as healthy or normal. The authors chose a relatively high threshold of 95% to emphasize the 5% of atypical cases that are particularly extreme.

Although some effects of IOP were more concentrated than others, the authors have shown that the concentration of responses was strong, irrespective of the measure analyzed, the population, or the percentile used to define a response as

typical. If using these predictions to determine whether the response to IOP of a particular ONH is typical or not, it is important to consider both the present study’s definition of typical and the uncertainty in the experimental measurements. Low density gradients (diffuse boundaries in the density plots of Figs. 3, 5, 6) indicate that the boundary of the region of typical response is sensitive to the percentile level but that the classification of a case is relatively insensitive to uncertainties in the experiment. Conversely, large density gradients (sharp boundaries) indicate that the boundary of the region of typical response would not change much if a different percentile level had been used to define typical, but that the classification of a case is highly sensitive to the uncertainties in the experiment.

Thirdly, whether a specific case was typical or not depended not only on the response used for the classification, but also on whether the decision was taken based on a single characteristic or two (Fig. 7). This was a consequence, again, of the complex nonlinear interactions between the parameters and the responses and emphasizes the importance of considering the multidimensional nature of the ONH response to variations in IOP.

The predictions of this study are in good agreement with the measurements (Kankipati L, et al. *IOVS* 2011;ARVO E-Abstract 6255)^{3,7,9-11} and predictions^{14,19,23,29} of acute effects of IOP on the human ONH. Agoumi and colleagues⁹ reported that for increases in IOP of about 12 mm Hg they observed LCD (with respect to Bruch’s membrane) between -8 and 8 μm. Kankipati and colleagues (Kankipati L, et al. *IOVS* 2011;ARVO E-Abstract 6255) reported changes in lamina position (measured with respect to Bruch’s membrane opening) between 164 μm anteriorly and 55 μm posteriorly. Levy and Crapps³ reported LCD between 0 and 20 μm posteriorly for IOP increases of 15 mm Hg. Yan and colleagues⁷ reported an LCD of 79 μm for an IOP increase of 45 mm Hg. Little is known about SCE in human eyes, except that the scleral canal

TABLE 3. Response Modes

Response	Mode (most likely response)	
	Uniform Population	Gaussian Population
LCD	LCD = 8.3 μm	LCD = 7.4 μm
SCE	SCE = 2.5 μm	SCE = 3.1 μm
LCD and SCE combined	LCD = 7.8 μm, SCE = 2.5 μm	LCD = 7.5 μm, SCE = 2.9 μm
Stress	Stress = 5.3 kPa	Stress = 5.7 kPa
Strain	Strain = 0.6%	Strain = 0.6%
Stress and Strain combined	Stress = 5.8 kPa, Strain = 0.48%	Stress = 5.7 kPa, Strain = 0.55%

These values are useful because an experimental measurement is most likely to obtain the mode.

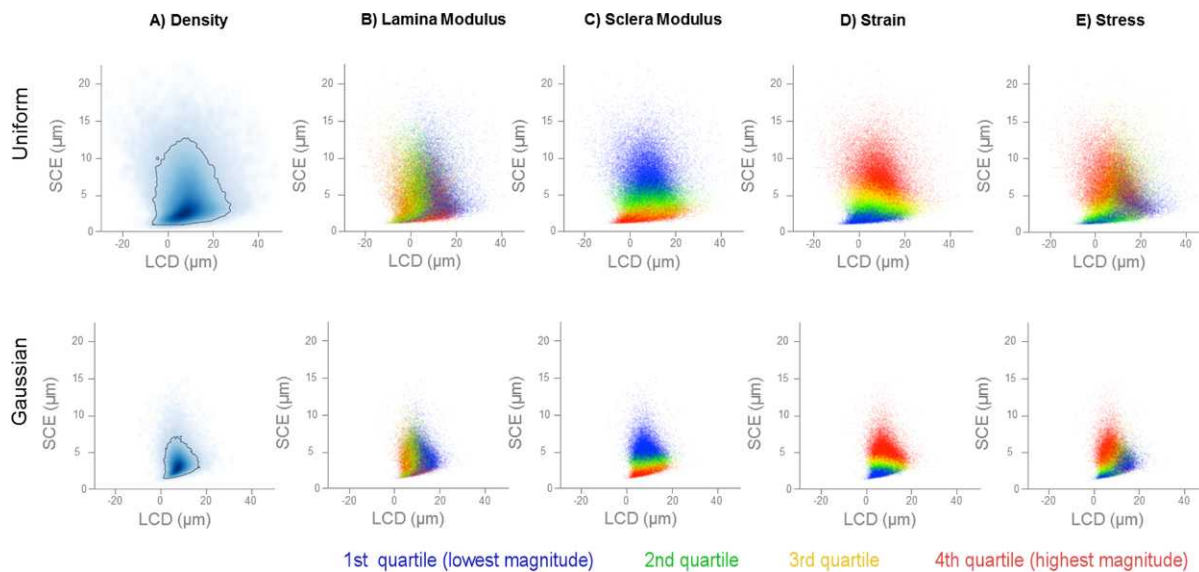


FIGURE 5. Two-dimensional distribution of LCD and SCE colored by factors and responses. Distributions of IOP-induced LCD and SCE for the uniform (*top row*) and Gaussian (*bottom row*) populations. The Panels in Column A are density plots repeated from Figure 3 to simplify comparisons with other Panels. The panels in columns B to E are colored by ONH parameters, namely the lamina modulus (**B**) or sclera modulus (**C**), or colored by two other aspects of the response to IOP, namely the tensile strain (**D**) or the stress (**E**) within the LC. Horizontal bands show how the sclera modulus affects SCE more strongly than LCD (**E**), and that the strain within the LC is much more closely associated with SCE than with LCD (**B**). The color bands were similar between the two populations, showing that the effects of lamina and sclera modulus did not depend on the population. There are some regions dominated by cases with high stress (*red points on the top left*, high SCE and low LCD, of plots in column E), or by cases with low stress (*blue points on the bottom right*, low SCE and high LCD, of plots in Column E). Still, there was still substantial overlap between the colors. Note how a stiff sclera resulted in reduced SCE and lamina strain, but did not affect LCD much.

diameters of contralateral eyes fixed at either 5 mm Hg or 50 mm Hg were more similar in contralateral eyes at different IOP than between unrelated eyes.¹⁰ The results of this study are also in reasonable agreement with measurements^{8,30-32} and predictions^{17,18,33,34} in animal models.

For this project numerical modeling presented several advantages over experiments: First, it allowed the authors to study many more ONHs than would have been possible in an experiment, increasing substantially the statistical power of the analysis. The 200,000 ONH models in this study also represented a much more detailed sampling of the parameter space than the authors' previous numerical sensitivity studies where typically a few hundred models were analyzed.^{13-15,23-25} The authors leveraged this to recalculate the strength of the factors influencing ONH biomechanics with high sensitivity to local nonlinearities and interactions. The present study found that the conclusions from the authors' previous sensitivity studies extend to large populations and were not determined by the sampling patterns. Second, unlike experiments, where only a few parameters of the ONH are known, all the characteristics of the numerical ONH models are known and were available for analysis to identify patterns of sensitivity to IOP. Despite recent advances in imaging technologies, such as deep-scanning OCT³⁵⁻⁴² and second harmonic imaging,^{43,44} it would not have been possible to evaluate the present study's hypothesis in an experiment. Third, numerical models allowed the authors to define the characteristics of the population of ONHs, such as the distributions of tissue geometries and mechanical properties. This is critical because the distributions of these characteristics of human ONHs are not completely known, and therefore it was important to test the extent to which the results depended on the characteristics of the population. The authors considered populations of ONHs with either uniform or Gaussian distribution of ONH characteristics. Gaussian distributions are potentially more realistic because they acknowledge the intuitive idea that more eyes are midrange than

extreme. Uniform distributions are simpler, without the case concentrations, and thus provide a reference with which to compare the results obtained using the Gaussian population. The authors found that the population had a slight effect, but did not determine the main results and therefore that the conclusions hold irrespective of the assumed population. Fourth, modeling allowed the investigators to determine IOP-induced stresses and strains, which represent the forces and deformations, respectively, induced within the tissues of the lamina by variations in IOP, which are not yet measurable in an experiment. These forces and deformations have been proposed to be related to the sensitivity of an ONH to variations in IOP,^{4,5,8,12,17-19,29,32,45} and therefore the authors believe that considering them raises the relevance of this analysis. The reported modeling approach allowed the authors to evaluate systematically the effects of various parameters, including geometry and mechanical properties, as well as their interactions. Some of the results, such as the odd shape of the regions of the typical response would have been difficult to predict without detailed parametric analysis because they arise from the complex nonlinear interaction of the responses and ONH characteristics. The authors found, for example, that there were no responses with very low stress or strain (Fig. 6), and further that the lowest stresses did not occur for the lowest strains and conversely that the lowest strains did not occur for the lowest stresses. This means that it would be atypical for an ONH to have simultaneously the lowest possible stresses and strains. From a more general perspective, stochastic modeling based on simplified generic models is subject to a similar but different set of assumptions and limitations than complex eye-specific models, which the authors have also studied.^{16-18,23,46} The results, therefore, provide a perspective that is unique and complementary to other modeling techniques.

Colloquially the term robust is sometimes used to mean that something is sturdy, strong, or stiff, meaning that it does not deform or fail under force. The authors use the term robust in a

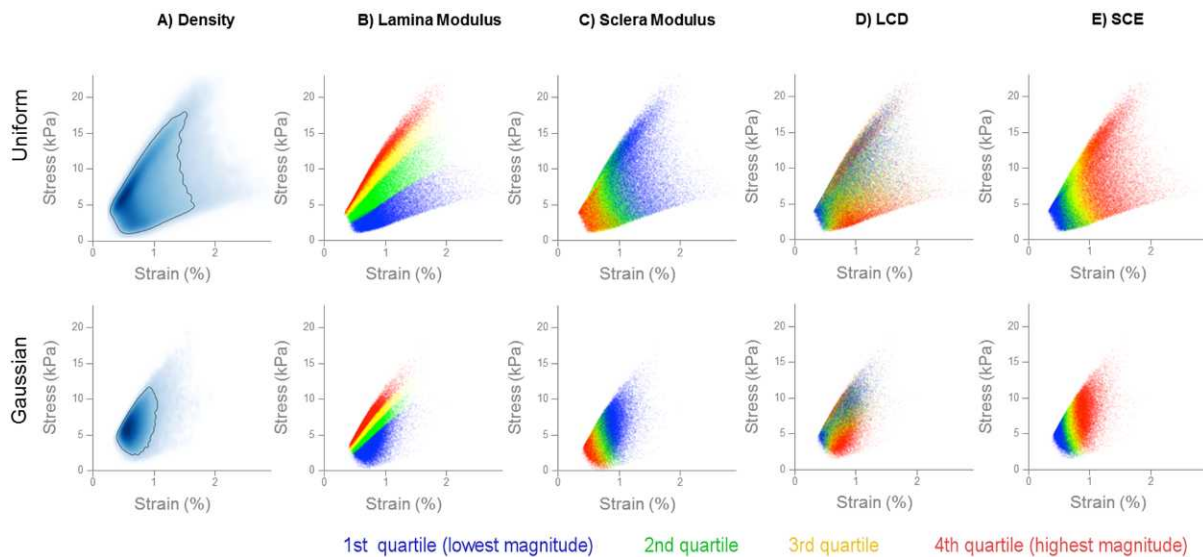


FIGURE 6. Two-dimensional distribution of stress and strain colored by factors and responses. Distributions of IOP-induced strain and stress within the LC for the uniform (*top row*) and Gaussian (*bottom row*) populations. The Panels in Column A are density plots repeated from Figure 3 to simplify comparisons with other Panels. The panels in columns B to E are colored by ONH parameters, namely the lamina modulus (**B**) or sclera modulus (**C**), or colored by two other aspects of the response to IOP, namely LCD (**D**) or SCE (**E**). The well-defined bands in the plot colored by lamina modulus (**B**) show how the relationship between lamina stress and strain depends strongly on the lamina modulus such that for the same strain a stiff lamina has higher stress than a compliant lamina. The color bands in the plots colored by sclera modulus show that both stress and strain are reduced when the sclera is stiff, with varying band widths indicating factor interactions. Interestingly, the color bands of sclera and lamina modulus are somewhat orthogonal, suggesting that variations in these parameters may suffice to determine the stress-strain response of a case. The boundaries of the response region were defined by the ranges of the lamina and sclera modulus. These boundaries were therefore sharper in the uniform population than in the Gaussian population. While the color bands are well defined in the plots colored by SCE, lamina modulus, and sclera modulus, the color pattern is nontrivial in the plots colored by LCD. This demonstrates a complex relationship between LCD and the stress and strain. The typical region has an interesting shape in the low stress and low strain region (*bottom left* of the scatter plots): The lowest strains did not occur for the lowest stresses, and the lowest stresses did not occur for the lowest strains. In this sense, an eye that could have been considered as the epitome of robustness, lowest strain and lowest stress, would be atypical. Similarly, the authors notice that the shape of the typical region shows that increases in either strain or stress would be accompanied by increases in the other.

more general sense, common in analysis of sensitivity and optimization,⁴⁷ to mean that the system can tolerate variations and perturbations while maintaining a relatively tight response envelope. This is an important distinction because the ONH, and in particular the scleral canal, is mechanically a weak spot in the sense that it deforms more under IOP than other ocular structures.

The effects of IOP were computed using surrogate models of the ONH that have been shown to approximate the predictions of the original finite element models very closely²² (for example, adjusted- R^2 s greater than 0.995). Surrogate models reduced considerably the time required for preprocessing, modeling, and analysis, allowing study of a large population of ONHs within a few minutes.

The authors have discussed in depth the assumptions and most salient consequences of this modeling and analysis, specifically the choice of model geometry and tissue mechanical properties,¹⁵ of the parameters and their ranges,^{13,14,23} and of the responses analyzed.^{13,14,16,23} Herein the authors present a summary of earlier discussions, with a focus on the limitations and considerations most relevant to this work.

The authors analyzed small increases in IOP (from 5–15 mm Hg) for several reasons: First, normal IOP is much more common than elevated IOP,^{1,48} and therefore the analysis is relevant to a larger group. Second, the authors' intent was to study the response of normal ONHs to variations in IOP, which is best accomplished by using geometries, tissue properties, and pressure variations within the normal range. Third, small IOP elevations may be particularly informative in understanding the pathogenesis of low-tension glaucoma. Whether the results of this study extend to nonnormal eyes seems

reasonable, but must be proven. Further, as the authors have demonstrated before, ONH biomechanics are complex, even with simplified geometries and material properties.^{13–16} Simulating a relatively small IOP increase allowed the authors to use linear material, whose stiffness can be specified by a single parameter for each tissue (the Young's modulus). Studies of ocular tissue properties have shown that while the assumption of a linearly elastic sclera is adequate at low levels of IOP, it becomes increasingly problematic at elevated IOP (typically above 20 mm Hg).^{29,33,49–52} The authors believe that a solid understanding of ONH biomechanics at low pressures helps build up for understanding larger pressure increases. The authors' models represent an acute increase in IOP and therefore the conclusions of this study should be interpreted as giving insight only into the acute effects of IOP and not into remodeling or aging processes.^{10–12,34,39,53–58}

The models in this study did not account for LC micro-architecture, which in humans is not fully characterized,⁴⁴ but that animal models suggest may alter the local levels of IOP-induced stress and strain (Kodiyalam S, et al. *IOVS* 2009;50:AR-VO E-Abstract 4893).^{17,18} The authors are developing FE models that incorporate more realistic anatomies (like the variations in scleral shell thickness⁵⁹), material properties (anisotropic and nonlinear scleral properties,^{29,33,49} lamina cribrosa anisotropy and inhomogeneity^{17,43,45}), and loading (larger IOP insult and cerebrospinal fluid pressure^{57,60–63}).

It is worth noting that some "natural" concentration of responses is to be expected in a well-behaved system (e.g., one which is not chaotic) such as the one under consideration. For example, in a simple 1D system it is natural to expect that 90% of the responses are concentrated in 90% of the response

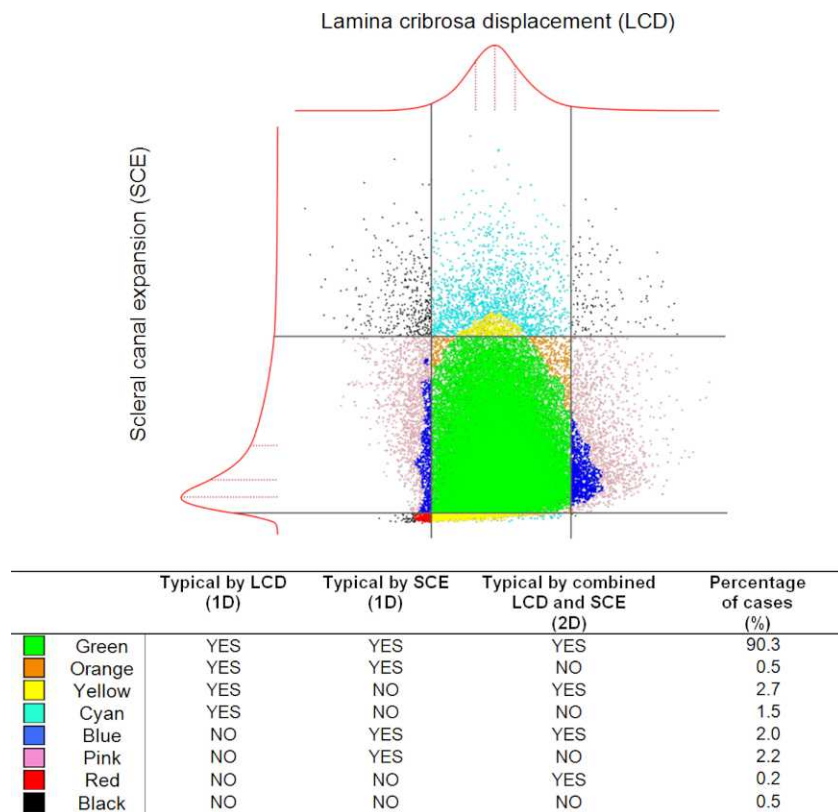


FIGURE 7. Comparison of 1D and 2D criteria to define a response as normal. The red lines are the distributions of LCD and SCE. The 1D distributions are marked with the 25, 50, and 75 percentiles (the quartiles in dotted red lines) as well as the 2.5 and 97.5 percentiles (grey lines) which were used to define typical in 1D. Using single or multiple responses to identify a response as typical led to different classifications of the cases. Some cases are classified as typical by only one criterion, some by both, and some by neither. The different regions are color coded and the criteria satisfied listed in the table below the plot. The authors' objective with this figure was to show that the classification of ONH responses as typical or atypical depends on the response used for classification, as well as whether a single response or two responses were used.

space, 80% of the responses in 80% of the response space, and so on and so forth, such that x fraction of the responses concentrates in x fraction of the response space. In 2D the effects are compounded such that x fraction of the responses concentrates in x² of the response space. In general, in an n dimensional space, the natural concentration of responses would be such that x fraction concentrates in xⁿ of the response space. The authors found that the responses computed in the present study were more concentrated than would be expected merely from the natural concentrations.

For the sake of generality the authors varied factors independently. It is possible that in vivo two or more input factors are correlated with one another; for example, studies in monkeys have suggested that thinner scleras tend to have higher stiffness.^{33,34} Such a covariation further supports this study's proposed framework of the eye as a robust biomechanical system. Other covariations could behave differently. This study's finding that various responses had similar patterns is consistent with results from a separate study in which the authors analyzed the covariances between responses (Sigal IA, Grimm JL, submitted, 2012). In summary, the authors have used numerical modeling to test the hypothesis that the eye is a robust biomechanical system, where the various factors determining the effects of IOP combine to produce a relatively stable response to IOP. The authors found support for this hypothesis in that despite wide variations in ONH characteristics and responses to IOP, some responses were much more

common than others. LCD and SCE, in particular, were highly concentrated. Within the framework that the authors propose, the complexity in the effects of IOP is an important property of the ONH which is necessary to understand if the scientific community is to be able to determine individual sensitivity to IOP. To the best of the authors' knowledge, this is also the first biomechanical analysis of a large population of ONHs.

References

1. Quigley HA. Glaucoma: macrocosm to microcosm the Friedenwald lecture. *Invest Ophthalmol Vis Sci.* 2005;46:2662-2670.
2. Balaratnasingam C, Morgan WH, Bass L, Matich G, Cringle SJ, Yu DY. Axonal transport and cytoskeletal changes in the lamellar regions after elevated intraocular pressure. *Invest Ophthalmol Vis Sci.* 2007;48:3632-3644.
3. Levy NS, Crapps EE. Displacement of optic nerve head in response to short-term intraocular pressure elevation in human eyes. *Arch Ophthalmol.* 1984;102:782-786.
4. Burgoyne CF, Downs JC, Bellezza AJ, Suh JK, Hart RT. The optic nerve head as a biomechanical structure: a new paradigm for understanding the role of IOP-related stress and strain in the pathophysiology of glaucomatous optic nerve head damage. *Prog Retin Eye Res.* 2005;24:39-73.
5. Sigal IA, Ethier CR. Biomechanics of the optic nerve head. *Exp Eye Res.* 2009;88:799-807.

6. Wilczek M. The lamina cribrosa and its nature. *Br J Ophthalmol*. 1947;31:551-565.
7. Yan DB, Coloma FM, Methetairaut A, Trope GE, Heathcote JG, Ethier CR. Deformation of the lamina cribrosa by elevated intraocular pressure. *Br J Ophthalmol*. 1994;78:643-648.
8. Yang H, Downs JC, Sigal IA, Roberts MD, Thompson H, Burgoyne CF. Deformation of the normal monkey optic nerve head connective tissue after acute IOP elevation within 3-D histomorphometric reconstructions. *Invest Ophthalmol Vis Sci*. 2009;50:5785-5799.
9. Agoumi Y, Sharpe GP, Hutchison DM, Nicoleta MT, Artes PH, Chauhan BC. Lamina and prelaminar tissue displacement during intraocular pressure elevation in glaucoma patients and healthy controls. *Ophthalmology*. 2011;118:52-59.
10. Sigal IA, Flanagan JG, Tertinegg I, Ethier CR. 3D morphometry of the human optic nerve head. *Exp Eye Res*. 2010;90:70-80.
11. Albon J, Purslow PP, Karwatowski WS, Easty DL. Age related compliance of the lamina cribrosa in human eyes. *Br J Ophthalmol*. 2000;84:318-323.
12. Grytz R, Sigal IA, Ruberti JW, Meschke G, Downs JC. Lamina cribrosa thickening in early glaucoma predicted by a microstructure motivated growth and remodeling approach. *Mech Mater*. 2012;44:99-109.
13. Sigal IA. Interactions between geometry and mechanical properties on the optic nerve head. *Invest Ophthalmol Vis Sci*. 2009;50:2785-2795.
14. Sigal IA, Flanagan JG, Ethier CR. Factors influencing optic nerve head biomechanics. *Invest Ophthalmol Vis Sci*. 2005;46:4189-4199.
15. Sigal IA, Flanagan JG, Tertinegg I, Ethier CR. Finite element modeling of optic nerve head biomechanics. *Invest Ophthalmol Vis Sci*. 2004;45:4378-4387.
16. Sigal IA, Flanagan JG, Tertinegg I, Ethier CR. Predicted extension, compression and shearing of optic nerve head tissues. *Exp Eye Res*. 2007;85:312-322.
17. Roberts MD, Liang Y, Sigal IA, et al. Correlation between local stress and strain and lamina cribrosa connective tissue volume fraction in normal monkey eyes. *Invest Ophthalmol Vis Sci*. 2010;51:295-307.
18. Roberts MD, Sigal IA, Liang Y, Burgoyne CF, Downs JC. Changes in the biomechanical response of the optic nerve head in early experimental glaucoma. *Invest Ophthalmol Vis Sci*. 2010;51:5675-5684.
19. Sander EA, Downs JC, Hart RT, Burgoyne CF, Nauman EA. A cellular solid model of the lamina cribrosa: mechanical dependence on morphology. *J Biomech Eng*. 2006;128:879-889.
20. Norman RE, Flanagan JG, Sigal IA, Rausch SM, Tertinegg I, Ethier CR. Finite element modeling of the human sclera: influence on optic nerve head biomechanics and connections with glaucoma. *Exp Eye Res*. 2011;93:4-12.
21. Girard MJ, Downs JC, Burgoyne CF, Suh JK. Peripapillary and posterior scleral mechanics-part I: development of an anisotropic hyperelastic constitutive model. *J Biomech Eng*. 2009;131:051011.
22. Sigal IA. An applet to estimate the IOP-induced stress and strain within the optic nerve head. *Invest Ophthalmol Vis Sci*. 2011;52:5497-5506.
23. Sigal IA, Flanagan JG, Tertinegg I, Ethier CR. Modeling individual-specific human optic nerve head biomechanics. Part II: influence of material properties. *Biomech Model Mechanobiol*. 2009;8:99-109.
24. Sigal IA, Yang H, Roberts MD, Burgoyne CF, Downs JC. IOP-induced lamina cribrosa displacement and scleral canal expansion: an analysis of factor interactions using parameterized eye-specific models. *Invest Ophthalmol Vis Sci*. 2011;52:1896-1907.
25. Sigal IA, Yang H, Roberts MD, et al. IOP-induced lamina cribrosa deformation and scleral canal expansion: independent or related? *Invest Ophthalmol Vis Sci*. 2011;52:9023-9032.
26. Montgomery DC. *Design and Analysis of Experiments*. Hoboken, NJ: Wiley; 2004;660.
27. R Development Core Team. R: a language and environment for statistical computing. R Foundation for Statistical Computing, Vienna, Austria. 2009; URL: <http://www.R-project.org>.
28. Artal P, Benito A, Tabernero J. The human eye is an example of robust optical design. *J Vis*. 2006;6:1-7.
29. Grytz R, Meschke G, Jonas JB. The collagen fibril architecture in the lamina cribrosa and peripapillary sclera predicted by a computational remodeling approach. *Biomech Model Mechanobiol*. 2011;10:371-382.
30. Fatehee N, Yu PK, Morgan WH, Cringle SJ, Yu DY. The impact of acutely elevated intraocular pressure on the porcine optic nerve head. *Invest Ophthalmol Vis Sci*. 2011;52:6192-6198.
31. Strouthidis NG, Fortune B, Yang H, Sigal IA, Burgoyne CF. Effect of acute intraocular pressure elevation on the monkey optic nerve head as detected by spectral domain optical coherence tomography. *Invest Ophthalmol Vis Sci*. 2011;52:9431-9437.
32. Bellezza AJ, Rintalan CJ, Thompson HW, Downs JC, Hart RT, Burgoyne CF. Anterior scleral canal geometry in pressurised (IOP 10) and non-pressurised (IOP 0) normal monkey eyes. *Br J Ophthalmol*. 2003;87:1284-1290.
33. Girard MJ, Downs JC, Bottlang M, Burgoyne CF, Suh JK. Peripapillary and posterior scleral mechanics-part II: experimental and inverse finite element characterization. *J Biomech Eng*. 2009;131:051012.
34. Girard MJ, Suh JK, Bottlang M, Burgoyne CF, Downs JC. Biomechanical changes in the sclera of monkey eyes exposed to chronic IOP elevations. *Invest Ophthalmol Vis Sci*. 2011;52:5656-5669.
35. Srinivasan VJ, Adler DC, Chen Y, et al. Ultrahigh-speed optical coherence tomography for three-dimensional and en face imaging of the retina and optic nerve head. *Invest Ophthalmol Vis Sci*. 2008;49:5103-5110.
36. Park SC, De Moraes CG, Teng CC, Tello C, Liebmann JM, Ritch R. Enhanced depth imaging optical coherence tomography of deep optic nerve complex structures in glaucoma. *Ophthalmology*. 2011;119:3-9.
37. Ivers KM, Li C, Patel N, et al. Reproducibility of measuring lamina cribrosa pore geometry in human and nonhuman primates with in vivo adaptive optics imaging. *Invest Ophthalmol Vis Sci*. 2011;52:5473-5480.
38. Girard MJ, Strouthidis NG, Ethier CR, Mari JM. Shadow removal and contrast enhancement in optical coherence tomography images of the human optic nerve head. *Invest Ophthalmol Vis Sci*. 2011;52:7738-7748.
39. Park HY, Jeon SH, Park CK. Enhanced depth imaging detects lamina cribrosa thickness differences in normal tension glaucoma and primary open-angle glaucoma. *Ophthalmology*. 2011;119:10-20.
40. Kagemann L, Ishikawa H, Wollstein G, et al. Ultrahigh-resolution spectral domain optical coherence tomography imaging of the lamina cribrosa. *Ophthalmic Surg Lasers Imaging*. 2008;39:S126-131.
41. Inoue R, Hangai M, Kotera Y, et al. Three-dimensional high-speed optical coherence tomography imaging of lamina cribrosa in glaucoma. *Ophthalmology*. 2009;116:214-222.
42. Yamanari M, Lim Y, Makita S, Yasuno Y. Visualization of phase retardation of deep posterior eye by polarization-sensitive swept-source optical coherence tomography with 1-microm probe. *Opt Express*. 2009;17:12385-12396.
43. Brown DJ, Morishige N, Neekhra A, Minckler DS, Jester JV. Application of second harmonic imaging microscopy to assess

- structural changes in optic nerve head structure ex vivo. *J Biomed Opt.* 2007;12:024029.
44. Winkler M, Jester B, Nien-Shy C, et al. High resolution three-dimensional reconstruction of the collagenous matrix of the human optic nerve head. *Brain Res Bull.* 2010;81:339-348.
 45. Roberts MD, Grau V, Grimm J, et al. Remodeling of the connective tissue microarchitecture of the lamina cribrosa in early experimental glaucoma. *Invest Ophthalmol Vis Sci.* 2009;50:681-690.
 46. Sigal IA, Flanagan JG, Tertinegg I, Ethier CR. Reconstruction of human optic nerve heads for finite element modeling. *Technol Health Care.* 2005;13:313-329.
 47. Nikolaidis E, Ghiocel DM, Singhal S. *Engineering Design Reliability Handbook.* Boca Raton, FL: CRC Press; 2004.
 48. Quigley HA. Number of people with glaucoma worldwide. *Br J Ophthalmol.* 1996;80:389-393.
 49. Grytz R, Meschke G. Constitutive modeling of crimped collagen fibrils in soft tissues. *J Mech Behav Biomed Mater.* 2009;2:522-533.
 50. Elsheikh A, Geraghty B, Alhasso D, Knappett J, Campanelli M, Rama P. Regional variation in the biomechanical properties of the human sclera. *Exp Eye Res.* 2010;90:624-633.
 51. Spoerl E, Boehm AG, Pillunat LE. The influence of various substances on the biomechanical behavior of lamina cribrosa and peripapillary sclera. *Invest Ophthalmol Vis Sci.* 2005;46:1286-1290.
 52. Myers KM, Coudrillier B, Boyce BL, Nguyen TD. The inflation response of the posterior bovine sclera. *Acta Biomater.* 2010;6:4327-4335.
 53. Morrison JC, Johnson EC, Cepurna W, Jia L. Understanding mechanisms of pressure-induced optic nerve damage. *Prog Retin Eye Res.* 2005;24:217-240.
 54. Hernandez MR. The optic nerve head in glaucoma: role of astrocytes in tissue remodeling. *Prog Retin Eye Res.* 2000;19:297-321.
 55. Crawford Downs J, Roberts MD, Sigal IA. Glaucomatous cupping of the lamina cribrosa: a review of the evidence for active progressive remodeling as a mechanism. *Exp Eye Res.* 2011;93:133-140.
 56. Yang H, Williams G, Downs JC, et al. Posterior (outward) migration of the lamina cribrosa and early cupping in monkey experimental glaucoma. *Invest Ophthalmol Vis Sci.* 2011;52:7109-7121.
 57. Jonas JB, Jonas SB, Jonas RA, Holbach L, Panda-Jonas S. Histology of the parapapillary region in high myopia. *Am J Ophthalmol.* 2011;152:1021-1029.
 58. Girard MJ, Suh JK, Bottlang M, Burgoyne CF, Downs JC. Scleral biomechanics in the aging monkey eye. *Invest Ophthalmol Vis Sci.* 2009;50:5226-5237.
 59. Norman RE, Flanagan JG, Rausch SM, et al. Dimensions of the human sclera: Thickness measurement and regional changes with axial length. *Exp Eye Res.* 2010;90:277-284.
 60. Berdahl JP, Allingham RR, Johnson DH. Cerebrospinal fluid pressure is decreased in primary open-angle glaucoma. *Ophthalmology.* 2008;115:763-768.
 61. Morgan WH, Yu DY, Alder VA, et al. The correlation between cerebrospinal fluid pressure and retrolaminar tissue pressure. *Invest Ophthalmol Vis Sci.* 1998;39:1419-1428.
 62. Morgan WH, Yu DY, Cooper RL, Alder VA, Cringle SJ, Constable IJ. The influence of cerebrospinal fluid pressure on the lamina cribrosa tissue pressure gradient. *Invest Ophthalmol Vis Sci.* 1995;36:1163-1172.
 63. Ren R, Jonas JB, Tian G, et al. Cerebrospinal fluid pressure in glaucoma: a prospective study. *Ophthalmology.* 2010;117:259-266.